Berezinskii-Kosterlitz-Thouless-like percolation transitions in the two-dimensional XY model

Hao Hu,[1] Youjin Deng,[1,*] and Henk W. J. Blöte[2,3]

[1]*Hefei National Laboratory for Physical Sciences at Microscale, Department of Modern Physics, University of Science
and Technology of China, Hefei 230027, China*

[2]*Instituut Lorentz, Leiden University, P. O. Box 9506, NL-2300 RA Leiden, The Netherlands*

[3]*Faculty of Applied Sciences, Delft University of Technology, P. O. Box 5046, NL-2600 GA Delft, The Netherlands*

We study a percolation problem on a substrate formed by two-dimensional XY spin configurations using Monte Carlo methods. For a given spin configuration, we construct percolation clusters by randomly choosing a direction x in the spin vector space, and then placing a percolation bond between nearest-neighbor sites i and j with probability $p_{ij} = \max(0, 1 - e^{-2Ks_i^x s_j^x})$, where $K > 0$ governs the percolation process. A line of percolation thresholds $K_c(J)$ is found in the low-temperature range $J \geqslant J_c$, where $J > 0$ is the XY coupling strength. Analysis of the correlation function $g_p(r)$, defined as the probability that two sites separated by a distance r belong to the same percolation cluster, yields algebraic decay for $K \geqslant K_c(J)$, and the associated critical exponent depends on J and K. Along the threshold line $K_c(J)$, the scaling dimension for g_p is, within numerical uncertainties, equal to 1/8. On this basis, we conjecture that the percolation transition along the $K_c(J)$ line is of the Berezinskii-Kosterlitz-Thouless type.

I. INTRODUCTION

The XY model is formulated in terms of two-dimensional spins $\vec{s}$ normalized as $|\vec{s}| = 1$ residing on the sites of a lattice. The reduced Hamiltonian of the XY model (already divided by $k_B T$, with k_B the Boltzmann constant and T the temperature) reads as

$$\mathcal{H} = -J \sum_{\langle ij \rangle} \vec{s}_i \cdot \vec{s}_j, \tag{1}$$

where the sum is over all nearest-neighbor pairs, and $J > 0$ is the ferromagnetic coupling strength. The spins are labeled by their site numbers.

It is known from the Mermin-Wagner-Hohenberg-Coleman theorem [1] that there can not exist spontaneous long-range order as long as J is finite in Eq. (1) because thermal fluctuations are strong enough to destroy the order. Nevertheless, the system undergoes a phase transition [2–4] as the coupling strength J increases. This type of transition is of infinite order and is known as the Berezinskii-Kosterlitz-Thouless (BKT) transition. For $J < J_c$, the spin-spin correlation function decays exponentially, and the spins form a plasma of vortices; but for $J > J_c$, the spin-spin correlation function decays algebraically with an exponent depending on J, and the spin configurations contain bound vortex-antivortex pairs. Transitions of the BKT type occur in various kinds of systems. The XY-type of transition is related by duality to roughening transitions in solid-on-solid and related models [5]. Apart from the XY model, BKT transitions are found, among others, in vertex models [6], models of crystal surfaces [7], the antiferromagnetic triangular Ising model [8], string theory [9], network systems [10], superfluid systems [11], and superconducting systems [12]. These models may involve long- or short-range interactions.

It is also known that certain observables of statistical models are equivalent or closely related to properly defined geometric quantities. For instance, the Potts model can be exactly mapped onto the random-cluster model [13], and the susceptibility χ of the former is related to the cluster-size distribution of the latter; a similar situation applies to the Nienhuis O(n) loop model [14] and the equivalent spin model [15]. The Mott-to-superfluid transition in the Bose-Hubbard model can be characterized by the winding number of the world lines of the particles [16]. The geometric percolation [17] process has been employed to study percolation on critical substrates, such as the Ising model [18–21], the Potts model [22–24], the O(n) model [25], and even quantum Hall systems [26].

In this paper, we study the percolation problem on the substrate of the XY model (1). There is still some freedom in the choice of the percolation criterion. For instance, one may place percolation bonds between all neighboring XY spins if their orientations differ less than a given angle called the "conducting angle". This problem was recently investigated by Wang *et al.* [27]. Here, we use a different criterion. For a given spin configuration, we choose a randomly oriented Cartesian reference frame (x, y) in the two-dimensional spin space, and place bonds between nearest-neighbor pairs, say sites i and j, with a probability

$$p_{ij} = \max\left(0, 1 - e^{-2Ks_i^x s_j^x}\right), \tag{2}$$

where $K > 0$ parametrizes the percolation problem. Note that, for $K = J$, these percolation clusters reduce to those formed by the cluster simulation process of the XY model as described in Sec. II.

The rest of this paper is organized as follows. Section III presents our numerical results for the critical points of the XY model on the square as well as on the triangular lattice. Section IV describes the analysis of the percolation problem for both lattices, with an emphasis on the determination of the

_____
*Corresponding author: yjdeng@ustc.edu.cn

universal character of this type of percolation transition. We conclude with a discussion in Sec. V.

II. ALGORITHM AND SAMPLED QUANTITIES

A. Spin-updating algorithm

We employ efficient Monte Carlo simulations of the XY model (1) by means of a cluster method [28,29]. We use a full cluster decomposition [28] as follows:

(1) Choose a randomly oriented Cartesian frame of reference (x, y) in the *spin* space, and project the spin along the x and y axes as $\vec{s} = s^x \hat{x} + s^y \hat{y}$. Accordingly, the scalar product in Eq. (1) is written $\vec{s}_i \cdot \vec{s}_j = s_i^x s_j^x + s_i^y s_j^y$, so that the Hamiltonian separates into two parts as $\mathcal{H} = \mathcal{H}_x + \mathcal{H}_y$, with $\mathcal{H}_x = -J \sum_{\langle ij \rangle} s_i^x s_j^x$ and similar for $\mathcal{H}_y$.

(2) Between each pair of nearest-neighboring sites, e.g., site i and j, place a bond with probability $p_{ij} = \max(0, 1 - e^{-2J s_i^x s_j^x})$.

(3) Construct clusters on the basis of the occupied bonds.

(4) Independently for each cluster, flip the x components of all the spins in the cluster with probability $1/2$.

B. Sampled quantities

We sampled several quantities, including the second and the fourth moments of the magnetization density $M^2 = |\sum_k \vec{s}_k|^2/V^2$ and $M^4 = |\sum_k \vec{s}_k|^4/V^4$. These quantities determine the dimensionless Binder ratio [30] as

$$Q_m = \langle M^2 \rangle^2 / \langle M^4 \rangle, \tag{3}$$

where $V = L^2$ is the volume. The susceptibility is $\chi = V \langle M^2 \rangle$.

Denoting the size of the ith cluster by C_i, we also sampled the second and the fourth moments of the cluster size distribution as

$$S_2 = \frac{1}{V^2} \sum_i C_i^2 \quad \text{and} \quad S_4 = \frac{1}{V^4} \sum_i C_i^4. \tag{4}$$

Accordingly, we define another dimensionless ratio as

$$Q_l = \langle S_2 \rangle^2 / \left(3 \langle S_2^2 \rangle - 2 \langle S_4 \rangle \right). \tag{5}$$

Note that for the Ising model, Q_l in Eq. (5) is equal to Q_m in Eq. (3).

Also, the spin-spin correlation $g_s(r)$ over distances $r = L/2$ and $L/4$ was sampled. A third dimensionless ratio Q_s is defined as

$$Q_s = \langle g_s(L/2) \rangle / \langle g_s(L/4) \rangle. \tag{6}$$

In the high-temperature range $J < J_c$, the spin-spin correlation decays exponentially, and Q_s goes to 0 as $L \to \infty$. At criticality, however, $g_s(r)$ tends to algebraic decay as r^{-2x_h}, and Q_s converges to a nontrivial universal value. In an ordered state with a nonzero magnetization density, Q_s would converge to 1 instead.

Finally, we define the correlation function $g_p(r)$ as the probability that two sites at a distance r belong to the same cluster. We sampled g_p over distances $r = L/2$ and $r = L/4$. The associated dimensionless ratio is

defined as

$$Q_p = \langle g_p(L/2) \rangle / \langle g_p(L/4) \rangle. \tag{7}$$

III. CRITICAL POINTS

A. Square lattice

We simulated the XY model on $L \times L$ square lattices with periodic boundary conditions, with system sizes in the range $4 \leqslant L \leqslant 1024$. As usual in Monte Carlo studies, the location of a critical point can well be determined using a dimensionless ratio. This is shown in Fig. 1 for the Binder ratio Q_m. For $J < J_c$, Q_m approaches the infinite-temperature value $1/2$ as $L \to \infty$, as expected for a normal distribution of the x and y components of the magnetization. For $J > J_c$, Q_m rapidly converges to a temperature-dependent value, as expected in the low-temperature XY phase.

Making use of the known magnetic scaling dimension $x_h = 1/8$ [4] at the BKT transition, and the logarithmic correction factor with exponent $1/8$ [4,31], we expect that the scaled quantity $\chi L^{2x_h - 2}(\ln L)^{-1/8}$ tends to a constant at the transition point. The intersections in Fig. 2, which shows this scaled quantity as a function of J for several system sizes, confirm this expectation.

Using the least-squares criterion, we fitted the quantity $\chi L^{2x_h - 2}(\ln L)^{-1/8}$ data by the formula

$$
\begin{aligned}
\chi L^{2x_h - 2}&(\ln L)^{-1/8} \\
&= a_0 + \sum_{i=1}^{3} a_i (J_c - J)^i (\ln L)^i + \sum_{j=1}^{2} r_j (J_c - J)^j \\
&\quad + b_1/(\ln L) + b_2 L^{-1} + b_3 L^{-2},
\end{aligned}
\tag{8}
$$

where the multiplicative and additive logarithmic corrections have been taken into account. We find that the data for $16 \leqslant L \leqslant 1024$ and $1.100 \leqslant J \leqslant 1.125$ are well described by Eq. (8). The fit yields $J_c = 1.124(3)$.

For the Ising model, one can prove that $\chi = V \langle M^2 \rangle = V \langle S_2 \rangle$, which exactly relates the thermodynamic quantity χ to the geometric quantity S_2. We thus expect that, in the case of
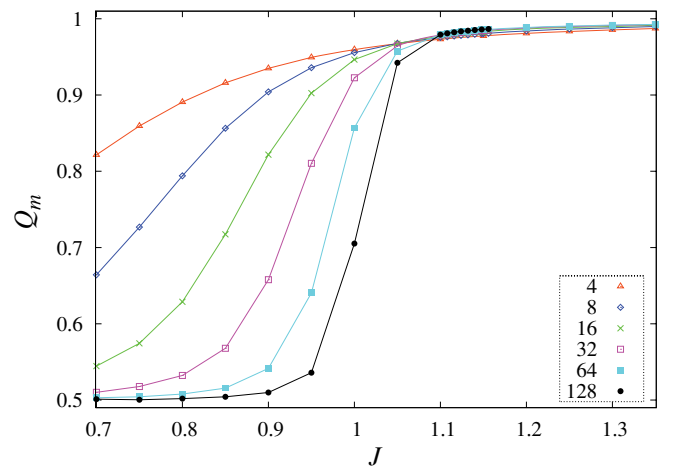

FIG. 1. (Color online) Binder ratio Q_m vs coupling strength J for the square lattice. The lines connecting data points are added for clarity.
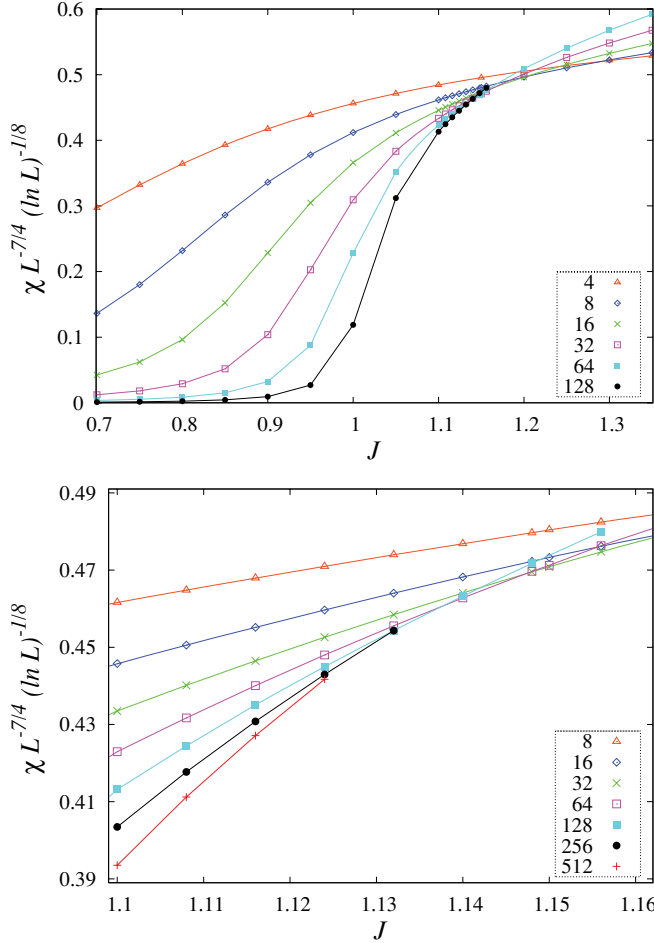
FIG. 2. (Color online) Scaled susceptibility $\chi L^{2x_h-2}(\ln L)^{-1/8}$ vs coupling strength J for the square lattice, with $x_h = 1/8$. The lower figure is an enlarged version, and includes data for $L = 256$ and 512. The lines connecting the data points are added for clarity.
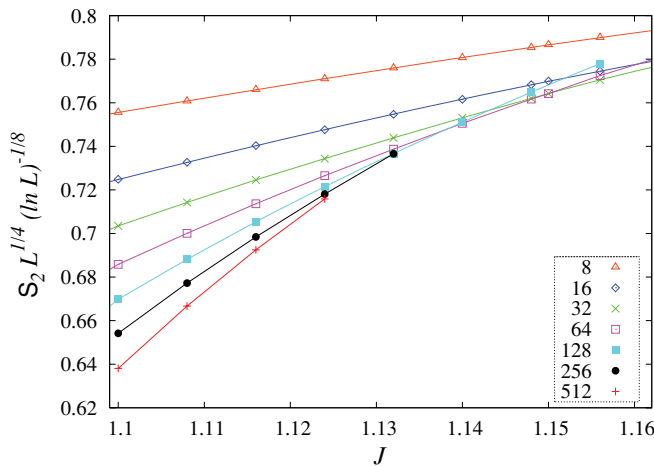

FIG. 3. (Color online) Scaled second moment $S_2 L^{2x_h}(\ln L)^{-1/8}$ of the cluster-size distribution vs coupling strength J. These results apply to the cluster decomposition of the spin model on the square lattice. The lines connecting the data points are added for clarity.
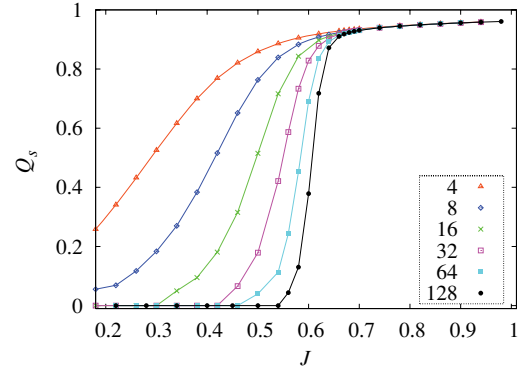

FIG. 4. (Color online) Ratio $Q_s = g_s(r = L/2)/g_s(r = L/4)$ vs coupling strength J for the triangular lattice, with g_s the spin-spin correlation. The lines connecting data points are added for clarity.

the XY model, the singularity of S_2 coincides with that of χ. The data for $S_2 L^{2x_h}(\ln L)^{-1/8}$ (shown in Fig. 3) were fitted by Eq. (8). This fit yields $J_c = 1.120(9)$, which is consistent with the result from χ.

There exist already many estimates for the critical point of the XY model on the square lattice, the latest of which are $J_c = 1.1199(1)$ by Hasenbusch and Pinn [32], $J_c = 1.1198(14)$ by Butera and Pernici [33], and $J_c = 1.1200(1)$ by Arisue [34]. Our result for J_c is consistent with these existing values.

B. Triangular lattice

We also simulated the XY model on the triangular lattice with periodic boundary conditions for linear system sizes L in the range $4 \leqslant L \leqslant 512$. The BKT phase transition is clearly exposed by Fig. 4, which plots the ratio $Q_s = g_s(r = L/2)/g_s(r = L/4)$ versus the coupling strength J. In the high-temperature range $J < J_c$, Q_s rapidly approaches zero, which reflects the absence of long-range correlations; in the low-temperature range $J > J_c$, it converges to a J-dependent value smaller than 1, in agreement with the presence of algebraically decaying correlations and the absence of a spontaneous magnetization.

The $g_s(L/2)L^{2x_h}(\ln L)^{-1/8}$ data near criticality are shown in Fig. 5. They were fitted by Eq. (8), which yielded $J_c = 0.6833(6)$. Analogous analyses were performed for the scaled susceptibility $\chi L^{2x_h-2}(\ln L)^{-1/8}$, leading to $J_c = 0.6831(6)$. Our results for the critical coupling are consistent with the latest result $J_c = 0.6824(8)$ by Butera and Pernici [33].

IV. PERCOLATION ANALYSIS

For each spin configuration generated by the Monte Carlo algorithm, we performed a full decomposition in percolation clusters, using the randomly oriented Cartesian frame in the spin space as chosen in the preceding Monte Carlo step, and then placed bonds between nearest-neighbor pairs with probabilities $p_{ij} = \max(0, 1 - e^{-2Ks_i^x s_j^x})$. The variable parameter $K > 0$ governs the percolation process. While these percolation clusters are not involved in spin updating, they reduce to those obtained during the cluster simulations in the
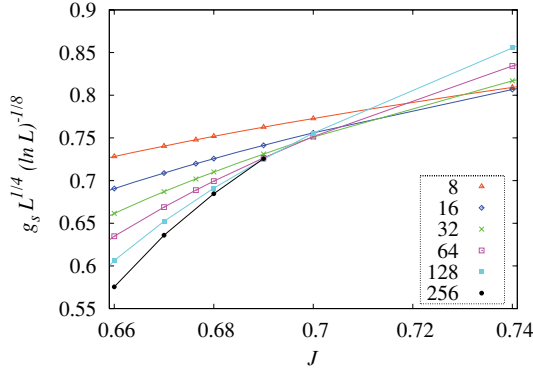
FIG. 5. (Color online) Scaled correlation $g_s(r = L/2)L^{2x_h}(\ln L)^{-1/8}$ vs coupling strength J for the triangular lattice, with $x_h = 1/8$. The lines connecting the data points are added for clarity.

case $K = J$. To analyze this percolation problem, we sampled several quantities, including the second and fourth moments S_2 and S_4 of the cluster-size distribution, the Binder ratio Q_l, the correlations $g_p(r = L/4)$, $g_p(r = L/2)$, and the ratio Q_p. In this section, we describe the numerical results and analyses, and also an exact result for this percolation problem on the triangular lattice.

A. Percolation on the square lattice

1. High-temperature range

For $\tanh K = 1$, i.e., in the limit $K \to \infty$, all pairs of nearest-neighbor spins are connected as long as their x components are pointing in the same direction. At zero coupling $J = 0$, spins at different sites are uncorrelated, so the percolation process reduces to the standard site-percolation process since the site occupation probability $p = 1/2$ may be identified with the random sign of s^x. An unimportant difference is that this process forms percolation clusters for all the lattice sites, while the standard site percolation constructs clusters only for the occupied sites. The site-percolation threshold p_c^s on the square lattice is very close to 0.592746 [35–37], and thus no infinite percolation cluster can occur at zero-coupling strength $J = 0$, even for $\tanh K = 1$. Furthermore, we mention that the zero-coupling fixed point $J = 0$ is attractive for the range $J < J_c$, which indicates that no percolation transition can occur for $0 \leqslant J < J_c$. This is in agreement with the results in Ref. [24], where a similar percolation problem was studied in the context of several Potts models. The expectation that a percolation transition is absent in the disordered phase of the square-lattice XY model was confirmed by Monte Carlo simulations that were performed at several couplings $0 < J < J_c$. Variation of K did not yield any signs of a percolation threshold.

2. Low-temperature range

The low-temperature XY phase $J \geqslant J_c$ displays algebraically decaying spin-spin correlations, which, unlike the exponential decay at $J < J_c$, allow the formation of a divergent percolation cluster for sufficiently large K. We may thus expect a percolation threshold to occur at a J-dependent value $K_c(J)$.
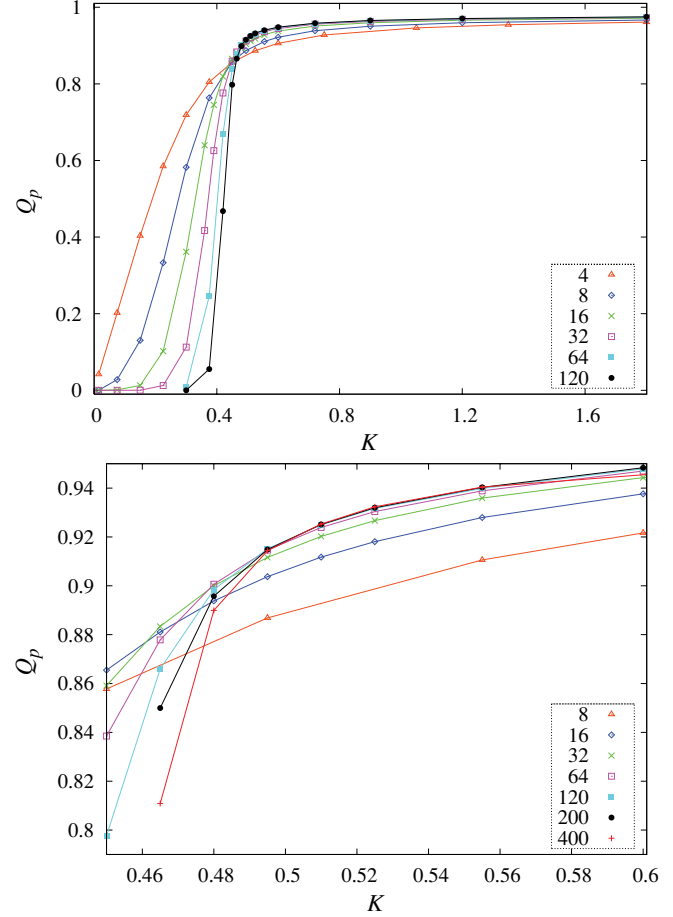

FIG. 6. (Color online) Dimensionless ratio Q_p vs the parameter K inducing the percolation transition. These data apply to the model on the square lattice, with the spin coupling $J = 3.0$. The lower figure is an enlarged version. The lines connecting the data points are added for clarity.

The existence of a percolation threshold $K_c(J)$ for $J > J_c$ is shown by the intersections of the curves in Fig. 6, which displays Q_p as a function of K at $J = 3.0$ for several L. These data show that $K_c(J = 3.0) \approx 0.505$. For $K < K_c(J)$, Q_p rapidly approaches zero, as expected from the absence of long-range correlations of $g_p(r)$.

In view of the long-range spin-spin correlations for $J \geqslant J_c$, we have no reason to expect that the percolation transition at the threshold $K_c(J)$ for $J > J_c$ belongs to the uncorrelated percolation universality class. This is supported by the observation that, at $J = J_c$, the fractal dimension of clusters with $K = J_c$ is $2 - x_h = 15/8$, which is different from the value $91/48$ for critical percolation clusters [38]. A closer look at the plot of Q_p versus K (Fig. 6) indicates that, for $K \geqslant K_c(J)$, Q_p rapidly converges to a K-dependent nontrivial value smaller than 1. We propose the interpretation that, like the thermal transition induced by the variation of J, the percolation transition induced by K is also BKT like.

In Fig. 7, we display the correlation g_p over a distance $r = L/2$ as a function of the linear system size L for several values of K. This figure shows a dependence of g_p on L that approaches power-law behavior for large L. This suggests that
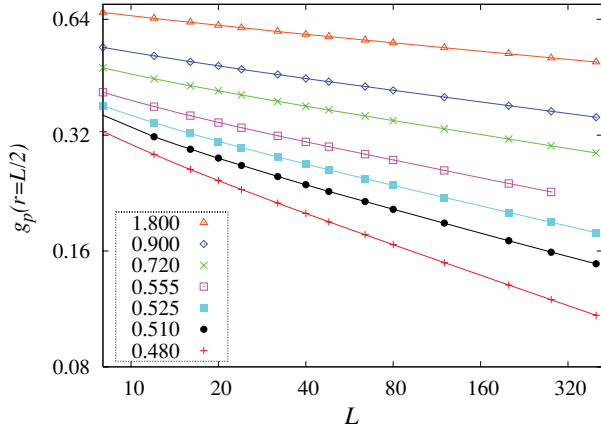
FIG. 7. (Color online) Correlation $g_p(L/2)$ vs linear system size L for several values of K, which are shown in the inset. The use of logarithmic scales displays the approximate power-law dependence on L. These data apply to the square-lattice XY model at $J = 3.0$. The lines connecting the data points are added for clarity.

percolation clusters remain critical for $K > K_c$. Furthermore the exponent governing the scaling of $g_p(r)$ appears to depend on K.

Next, we fitted the $g_p(r = L/2)$ data at $J = 3.0$ by

$$g_p = L^{-2x_h}(g_0 + g_1 L^{-1} + g_2 L^{-2}),   (9)$$

where x_h is the associated scaling dimension. The terms with g_1 and g_2 describe the finite-size corrections, and the correction exponents are simply set at -1 and -2, respectively. The results are shown in Table I.

We conjecture that the fractal dimension $2 - x_h$ of the percolation clusters at $K_c(J)$ assumes the exact BKT value with $x_h = 1/8$. This conjecture is based on the BKT-like behavior of the percolation transition in the low-temperature range, and on the numerical evidence for x_h obtained from the correlation $g_p(r = L/2)$ in Table I. First, the percolation in the low-temperature range seems to be BKT like. Second, the fit results for the scaling dimension x_h, when interpolated to K_c as given in Table II, yield a value close to $1/8$. The data for the scaled quantity $g_p(r = L/2)L^{1/4}(\ln L)^{-1/8}$, shown in Fig. 8 for $J = 3.0$, confirm the existence of intersections, apparently converging to the same value of K as those in Fig. 6. Furthermore, we found that the data for $g_p(r = L/2)$ in

TABLE I. Results for the scaling dimension x_h at $J = 3.0$ for various values of K for the square lattice. Parameters $L_{\min}$ and $L_{\max}$ are the minimum and the maximum system size between which the Monte Carlo data of g_p are included in the fit.

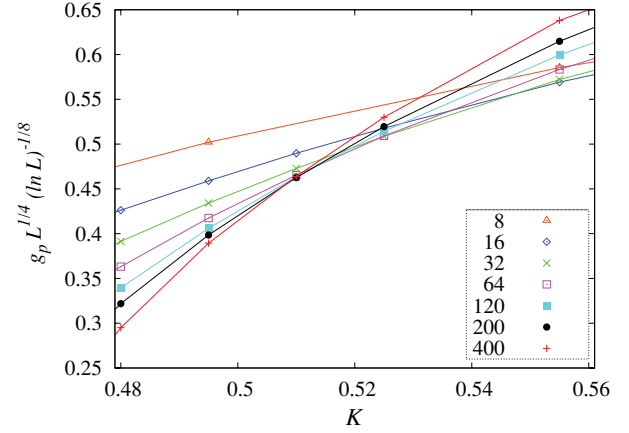| K	3.0	1.8	1.2	0.9	0.72
$L_{\min}$	20	20	16	16	12
$L_{\max}$	400	400	400	400	400
x_h	0.02916(2)	0.0345(6)	0.0412(6)	0.0492(6)	0.0590(6)
K	0.60	0.555	0.525	0.510	0.495
$L_{\min}$	16	16	16	16	16
$L_{\max}$	400	400	400	400	400
x_h	0.0751(6)	0.0857(6)	0.0990(6)	0.1108(6)	0.1290(8)

FIG. 8. (Color online) Scaled correlation $g_p L^{1/4}(\ln L)^{-1/8}$ over a distance $r = L/2$ vs K for various linear system size L shown in the inset. These data apply to the square-lattice XY model at $J = 3.0$. The lines connecting the data points are added for clarity.

the interval $0.47 \leqslant K \leqslant 0.515$ at $J = 3.0$ are well described by Eq. (8) for finite sizes in the range $32 \leqslant L \leqslant 400$. This fit yields an estimate for the percolation threshold at $K_c(J = 3.0) = 0.504(8)$.

We also performed simulations at $J = 2.4, 1.8, 1.4$, and 1.2, and observe a behavior similar to that described above for $J = 3.0$. On the basis of a fit of the $g_p L^{1/4}(\ln L)^{-1/8}$ data by Eq. (8), we obtain the associated percolation thresholds, which are shown in Table II. Next, we fitted Eq. (9) to the $g_p(r = L/2)$ data at various points (J, K) for $J \geqslant J_c$ and $K \geqslant K_c(J)$. The results are shown in Table III.

In addition, we carried out simulations at $J = 1.12$, very close to the thermal critical point $J_c = 1.124(3)$. The ratio $Q_p(K)$ appears to behave similarly as in Fig. 6, which suggests a BKT-like percolation transition. The estimated threshold $K_c = 1.120(9)$ agrees with the critical point J_c. This fits well with the continuation of the $K_c(J)$ line in Fig. 9. Further, the numerical result for the fractal dimension of the
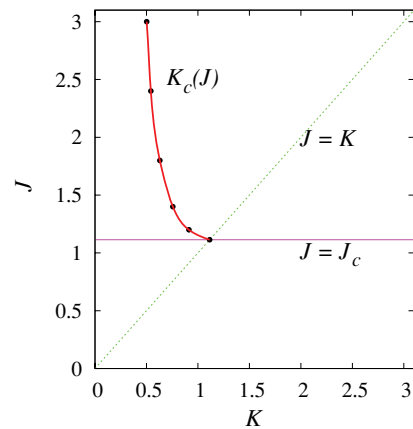

FIG. 9. (Color online) Phase diagram of the square-lattice XY model in the J-K parameter space. The horizontal line represents the thermal BKT transition, and the diagonal line applies to $K = J$, where the percolation clusters are just those formed by the cluster algorithm. The line connecting the data points is added for clarity.

TABLE II. Percolation threshold $K_c(J)$ for various values of the XY coupling strength J.

Square	J	3.0	2.4	1.8	1.4	1.2	1.12
	K_c	0.504(8)	0.553(5)	0.646(9)	0.785(9)	0.946(8)	1.120(9)
Triangular	J	2.2	1.8	1.4	1.0	0.8	0.6824
	K_c	0.300(3)	0.310(1)	0.356(4)	0.424(9)	0.520(9)	0.675(9)

percolation clusters at $K = J_c$ is consistent with the BKT value $2 - x_h = 15/8$.

The results in Tables II and III are summarized in Figs. 9 and 10, respectively.

B. Percolation on the triangular lattice

1. Matching property

The matching property [39,40] plays an important role in the determination of the site-percolation thresholds of several two-dimensional lattices; here we briefly review this subject. For a given planar lattice $\mathcal{P} \equiv (\mathcal{V}, \mathcal{B})$, where $\mathcal{V}$ is the set of lattice sites and $\mathcal{B}$ is the edge set, one does the following: (1) Select parts of the faces of $\mathcal{P}$, and fill in all the "diagonals" in those faces. This yields the lattice $\mathcal{L} \equiv (\mathcal{V}, \mathcal{B} + \mathcal{A})$, where $\mathcal{A}$ represents the set of all added diagonal edges. (2) Select the faces that are not picked up in step (1), and fill in all the diagonals in these faces. One then has the lattice $\mathcal{L}^* \equiv (\mathcal{V}, \mathcal{B} + \mathcal{A}^*)$, with $\mathcal{A}^*$ the set of diagonals drawn in step (2). Lattices $\mathcal{L}$ and $\mathcal{L}^*$ are matching to each other; note that $\mathcal{L}$ and $\mathcal{L}^*$ may be nonplanar. Since no "diagonal" can be filled in a triangle, the triangular lattice is self-matching. It can be shown that, for the site-percolation problem, the cluster numbers per

site $\kappa(p)$ and $\kappa^*(1 - p)$ on a pair of matching lattices $\mathcal{L}$ and $\mathcal{L}^*$ satisfy

$$\kappa(p) - \kappa^*(1 - p) = \phi(p), \tag{10}$$

where p is the site-occupation probability and $\phi(p)$ is a finite polynomial (it is termed "matching polynomial"). Equation (10) indicates that, if the cluster-number density κ on the lattice $\mathcal{L}$ exhibits a singularity at a site-occupation probability p, the same singularity will also occur in κ^* on $\mathcal{L}^*$ at $1 - p$. Together with the plausible assumption that there is only one transition, the matching argument yields that the percolation threshold is $p_c = 1/2$ for all self-matching lattices like the triangular lattice; further, it requires that $\phi(p = 1/2) = 0$, which is indeed satisfied by the result [40] $\phi(p) = p(1 - p)(1 - 2p)$ for self-matching lattices. An important feature of the matching argument is that it is still valid in the presence of interactions, as long as these interactions are symmetrical under the interchange of occupied and unoccupied sites.

2. Percolation at $\tanh K = 1$

As mentioned in Sec. IV A 1, the case $\tanh K = 1$, $J = 0$ in this percolation process corresponds with the case $p = 1/2$

TABLE III. Results for the scaling dimension x_h at various points (J, K) for the square lattice.

| $J = 3.0$	K	3.0	1.8	1.2	0.9	0.72
	x_h	0.02916(2)	0.0345(6)	0.0412(6)	0.0492(6)	0.0590(6)
	K	0.60	0.555	0.525	0.510	0.495
	x_h	0.0751(6)	0.0857(6)	0.0990(6)	0.1108(6)	0.1290(8)
$J = 2.4$	K	2.4	1.44	1.2	0.96	0.84
	x_h	0.03748(5)	0.0460(6)	0.0491(6)	0.0560(6)	0.0628(6)
	K	0.72	0.648	0.60	0.576	0.552
	x_h	0.0719(6)	0.0821(6)	0.0925(6)	0.1010(6)	0.1151(6)
$J = 1.8$	K	1.8	1.26	1.08	0.9	0.81
	x_h	0.05282(5)	0.0614(6)	0.0672(6)	0.0759(6)	0.0832(6)
	K	0.72	0.684	0.666	0.648	
	x_h	0.0954(6)	0.1028(6)	0.1069(6)	0.1140(6)	
$J = 1.4$	K	1.4	1.19	0.98	0.854	0.798
	x_h	0.07386(5)	0.0805(6)	0.0915(6)	0.1033(6)	0.1125(6)
	K	0.784	0.77	0.756		
	x_h	0.1157(6)	0.1202(6)	0.1250(6)		
$J = 1.2$	K	1.8	1.44	1.2	1.14	1.08
	x_h	0.0798(6)	0.0873(6)	0.09610(6)	0.0988(6)	0.1028(6)
	K	1.02	0.96			
	x_h	0.1084(6)	0.1159(6)			
$J = 1.12$	K	3.0	2.5	2.0	1.5	1.21
	x_h	0.0784(3)	0.0821(3)	0.0876(4)	0.0984(5)	0.1108(3)
	K	1.18	1.15			
	x_h	0.1132(3)	0.1162(5)			
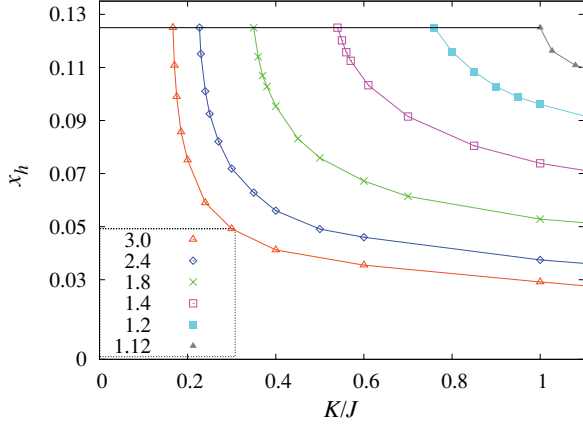
FIG. 10. (Color online) Scaling dimension x_h for percolation clusters at various points (J,K) for the square lattice. The values of J are shown in the inset. The horizontal line is located at $x_h = 1/8$ and corresponds with the critical line $K_c(J)$. This figure indicates that the scaling dimension x_h depends on K as well as on J, and approaches $1/8$ for $K \to K_c(J)$. The lines connecting the data points are added for clarity.

for the standard-site percolation. The standard-site-percolation threshold for the triangular lattice is $p_c = 1/2$; thus, the percolation threshold of this percolation problem at $J = 0$ is $\tanh K = 1$.

Since the matching argument is independent of the coupling J, and no spontaneous symmetry breaking occurs in the two-dimensional XY model, $\tanh K = 1$ describes a critical line for finite J. Further, we expect that, in the high-temperature range $J < J_c$, the percolation transition is in the universality class of standard uncorrelated percolation, since there is no long-range spin-spin correlation.

Figure 11 shows the data for the ratio Q_l, which is defined by Eq. (5) on the basis of the size distributions of the percolation clusters. For $J > J_c$, Q_l approaches a J-dependent value that is clearly smaller than 1. This implies the absence of an infinite cluster that occupies a finite fraction of the whole lattice. The singularity at the thermal transition point J_c is reflected by the jump that develops near $J_c \approx 0.68$.
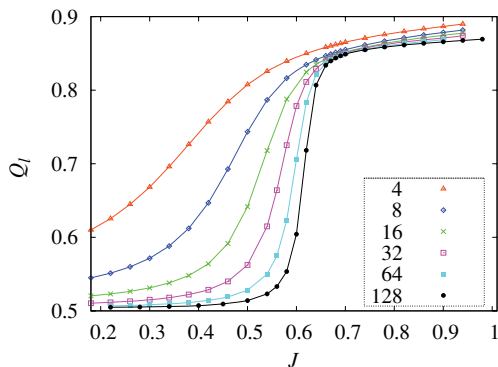

FIG. 11. (Color online) Ratio Q_l vs coupling strength J for the triangular lattice at $\tanh K = 1$. The lines connecting the data points are added for clarity.
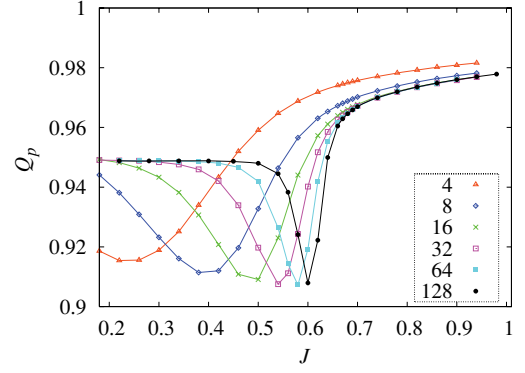

FIG. 12. (Color online) Ratio Q_p vs coupling strength J on the triangular lattice at $\tanh K = 1$. The lines connecting the data points are added for clarity.

Figure 12 shows the data for the ratio Q_p. For $J < J_c$, Q_p converges to a universal value $Q_{pc} \approx 0.95$ [note that this value differs from $Q_{pc} = 0.872776(3)$ [41] for standard percolation on the triangular lattice, due to the difference mentioned in the first paragraph of Sec. IV A 1]. For $J > J_c$, Q_p approaches a J-dependent value smaller than 1; we thus expect that the correlation $g_p(r)$ decays algebraically rather than exponentially. The thermal transition at J_c is reflected by the rapid variation of Q_p near $J_c \approx 0.68$ for large L.

The data for the scaled correlation $g_p(L/2)$ at $\tanh K = 1$ are shown in Fig. 13 as a function of J, with $x_h = 5/48$ for the uncorrelated percolation universality. The convergent behavior for $J < J_c$ as a function of L confirms that the transition in this range belongs to the standard percolation universality class. The intersections roughly represent the thermal transition point J_c.

3. Percolation at $\tanh K \neq 1$

Following similar procedures as in Sec. IV A, we obtain a percolation line $K_c(J)$ in the low-temperature range $J > J_c$ for the triangular lattice. For $J < J_c$, we do not find a percolation threshold at finite values of K. The numerical
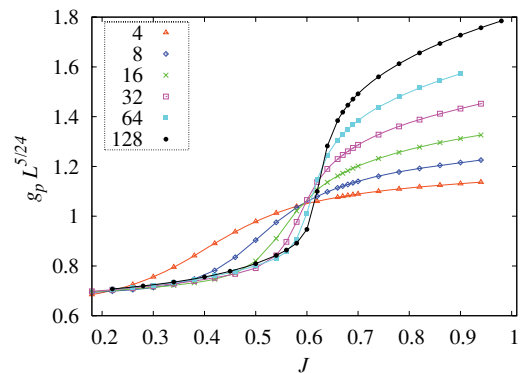

FIG. 13. (Color online) Scaled correlation $g_p(L/2)L^{2x_h}$ vs coupling strength J for the triangular lattice at $\tanh K = 1$, with $x_h = 5/48$, which applies to the uncorrelated percolation universality class. The lines connecting the data points are added for clarity.
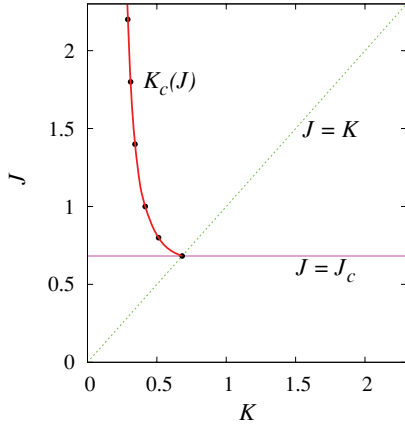
FIG. 14. (Color online) Phase diagram in the J-K parameter space for the XY model on the triangular lattice. The horizontal line is the thermal BKT transition, and the diagonal line is for $K = J$, where the percolation clusters are just those formed by the Monte Carlo cluster algorithm. In addition, there is a percolation line for $J < J_c$ at $\tanh K = 1$, outside the range of this figure. The line connecting the data points is added for clarity.

results are shown in Table II and Fig. 14. It is observed that the percolation in the range $J > J_c$ is also BKT like, with a fractal dimension $2 - x_h = 15/8$ at $K_c(J)$, and a scaling dimension x_h depending on parameters K and J in the range $K > K_c(J)$. This is consistent with the results for the square lattice in Sec. IV A.

V. DISCUSSION

Since spins in the same cluster formed during the simulations must have x components of the same sign, the absence of a spontaneous magnetization [1] in the XY model means that the density of the largest cluster in the thermodynamic limit is also restricted to be zero, at least for finite values of J. The same restriction thus applies to percolation clusters formed with $K = J$ in Eq. (2), and it must also hold for $K < J$. The absence of a nonzero density of the largest percolation cluster is in agreement with the interpretation of the percolation transitions for $K < J$ described in Sec. IV as BKT like.

The results presented in Sec. IV A for the square lattice include a line $K_c(J)$ of percolation thresholds for $J > J_c$. Also, for $J = J_c$, $K > J_c$, there is a line of percolation thresholds, analogous to those found for the Ising [20] and the Potts [22] models. The result that the percolation clusters remain critical in the whole region $J > J_c$, $K > K_c(J)$ is, however, markedly different from the Ising and Potts cases. Furthermore, we found that, as can be seen from the data points for $J = 1.12 \approx J_c$ in Fig. 10, the magnetic exponent depends on K along the latter line, which is thus a "nonuniversal" line of percolation transitions, where the bond dilution field parametrized by K is truly marginal. The existence of a BKT transition induced by varying K at the point $K = J = J_c$ corresponds with a marginally relevant bond-dilution field in the $K < J_c$ direction. The absence of a percolation line $K_c(J)$ for $J < J_c$ is in agreement with the argument given in Sec. IV A.

As mentioned earlier, for the triangular lattice with $J < J_c$, the line $\tanh K = 1$ is critical, and belongs to the standard-percolation universality class. The continuation of the $\tanh K = 1$ line to $J \geqslant J_c$ is also critical (in the sense that the correlation functions display algebraic decay), but with a J-dependent critical exponent.

In order to obtain some more information on the dependence of the present percolation problem on the coordination number z, we also simulated the $z = 18$ equivalent-neighbor XY model on the triangular lattice, which has equal nearest-, second-nearest-, and third-nearest-neighbor interactions. The procedure outlined in Sec. III yielded an estimate of the thermal transition at $J_c = 0.162(2)$. As expected, a Monte Carlo analysis of the percolation problem with $z = 18$ showed the existence of a critical line $K_c(J)$ in the high-temperature phase $J < J_c$ belonging to the standard-percolation universality class. When J approaches J_c, the $K_c(J)$ line bends toward large values of K. This suggests that the $K_c(J)$ line ends at $K \to \infty$ for $J = J_c$. For $K > K_c(J)$, there is clear evidence for the existence of a percolation cluster with a finite density in the limit of large L.

In the low-temperature range $J > J_c$, we found, just as for the models with nearest-neighbor interactions, a BKT-like transition line $K_c(J)$, as in Figs. 9 and 14. In spite of the relatively large coordination number $z = 18$, no evidence is found for a percolation cluster of a nonzero density, even at $\tanh K = 1$. Although the spin-spin correlations in the algebraic XY phase for $J > J_c$ stimulate the percolation transition in the sense that it occurs at smaller values of K when J increases, it also appears that they obstruct the formation of a percolation cluster with a nonzero density.

Aside from the rule based on Eq. (2), other procedures for placing bonds may be applied. For instance, as mentioned in the Introduction, Wang *et al.* [27] placed percolation bonds between neighboring XY spins if their orientations differ less than a given threshold, and found percolation transitions in the uncorrelated percolation universality class for all XY couplings. Another possibility is to place percolation bonds with probabilities given, instead of Eq. (2), by $p_{ij} = \max(0, 1 - e^{-2K\vec{s}_i \cdot \vec{s}_j})$. In that case, we expect percolation transitions similar to those of Ref. [27], including transitions in the low-temperature range $J > J_c$ of the XY model. Indeed, a preliminary Monte Carlo analysis of this problem [42] confirms the existence of such transitions in the universality class of uncorrelated percolation.

Finally, we remark that recently a percolation problem was formulated on the basis of the O(n) loop configurations [25]. Since the XY model is equivalent with the O(2) model, another way thus arises to introduce percolation in XY-type models. Although this seems to be a very different approach, it reproduces our result that a marginally relevant dilution field exists at the BKT transition.

[1] N. D. Mermin and H. Wagner, Phys. Rev. Lett. **17**, 1133 (1966); N. D. Mermin, J. Math. Phys. **8**, 1061 (1967); P. C. Hohenberg, Phys. Rev. **158**, 383 (1967) ; S. Coleman, Commun. Math. Phys. **31**, 259 (1973).

[2] V. L. Berezinskii, Zh. Eksp. Teor. Fiz. **59**, 907 (1970) [Sov. Phys. JETP **32**, 493 (1971)].

[3] J. M. Kosterlitz and D. J. Thouless, J. Phys. C **5**, L124 (1972); **6**, 1181 (1973).

[4] J. M. Kosterlitz, J. Phys. C **7**, 1046 (1974).

[5] J. V. José, L. P. Kadanoff, S. Kirkpatrick, and D. R. Nelson, Phys. Rev. B **16**, 1217 (1977).

[6] E. H. Lieb and F. Y. Wu, in *Phase Transitions and Critical Phenomena*, edited by C. Domb and M. S. Green (Academic, London, 1972), Vol. 1.

[7] H. van Beijeren, Phys. Rev. Lett. **38**, 993 (1977).

[8] B. Nienhuis, H. J. Hilhorst, and H. W. J. Blöte, J. Phys. A **17**, 3559 (1984); X.-F. Qian and H. W. J. Blöte, Phys. Rev. E **70**, 036112 (2004).

[9] M. Maggiore, Nucl. Phys. B **647**, 69 (2002).

[10] M. Bauer, S. Coulomb, and S. N. Dorogovtsev, Phys. Rev. Lett. **94**, 200602 (2005); M. Hinczewski and A. N. Berker, Phys. Rev. E **73**, 066126 (2006); E. Khajeh, S. N. Dorogovtsev, and J. F. F. Mendes, *ibid.* **75**, 041112 (2007); A. N. Berker, M. Hinczewski, and R. R. Netz, *ibid.* **80**, 041118 (2009).

[11] D. J. Bishop and J. D. Reppy, Phys. Rev. Lett. **40**, 1727 (1978).

[12] D. J. Resnick, J. C. Garland, J. T. Boyd, S. Shoemaker, and R. S. Newrock, Phys. Rev. Lett. **47**, 1542 (1981).

[13] P. W. Kasteleyn and C. M. Fortuin, J. Phys. Soc. Jpn. (Suppl.) **26**, 11 (1969); C. M. Fortuin and P. W. Kasteleyn, Physica (Amsterdam) **57**, 536 (1972).

[14] B. Nienhuis, Phys. Rev. Lett. **49**, 1062 (1982); J. Stat. Phys. **34**, 731 (1984).

[15] E. Domany, D. Mukamel, B. Nienhuis, and A. Schwinger, Nucl. Phys. B **190**, 279 (1981).

[16] E. L. Pollock and D. M. Ceperley, Phys. Rev. B **36**, 8343 (1987).

[17] D. Stauffer and A. Aharony, *Introduction to Percolation Theory* (Taylor and Francis, London, 1994), 2nd ed.; G. Grimmett, *Percolation* (Springer, Berlin, New York, 1999), 2nd ed.

[18] M. F. Sykes and D. S. Gaunt, J. Phys. A **9**, 2131 (1976).

[19] A. Coniglio, C. R. Nappi, F. Peruggi, and L. Russo, J. Phys. A **10**, 205 (1977).

[20] A. Coniglio and W. Klein, J. Phys. A **13**, 2775 (1980).

[21] Y. Deng and H. W. J. Blöte, Phys. Rev. E **70**, 056132 (2004).

[22] A. Coniglio and F. Peruggi, J. Phys. A **15**, 1873 (1982).

[23] Y. Deng, H. W. J. Blöte, and B. Nienhuis, Phys. Rev. E **69**, 026123 (2004).

[24] X.-F. Qian, Y. Deng, and H. W. J. Blöte, Phys. Rev. B **71**, 144303 (2005).

[25] C.-X. Ding, Y. Deng, W.-A. Guo, and H. W. J. Blöte, Phys. Rev. E **79**, 061118 (2009).

[26] D.-H. Lee, Z. Wang, and S. Kivelson, Phys. Rev. Lett. **70**, 4130 (1993).

[27] Y. Wang, W.-A. Guo, B. Nienhuis, and H. W. J. Blöte, Phys. Rev. E **81**, 031117 (2010).

[28] R. H. Swendsen and J. S. Wang, Phys. Rev. Lett. **58**, 86 (1987).

[29] U. Wolff, Phys. Rev. Lett. **60**, 1461 (1988).

[30] K. Binder, Z. Phys. B **43**, 119 (1981).

[31] D. J. Amit, Y. Y. Goldschmidt, and G. Grinstein, J. Phys. A **13**, 585 (1980); L. P. Kadanoff and A. B. Zisook, Nucl. Phys. B **180**, 61 (1981); R. Kenna, e-print arXiv:cond-mat/0512356 (2005).

[32] M. Hasenbusch and K. Pinn, J. Phys. A **30**, 63 (1997); M. Hasenbusch, *ibid.* **38**, 5869 (2005).

[33] P. Butera and M. Pernici, Physica A (Amsterdam) **387**, 6293 (2008).

[34] H. Arisue, Phys. Rev. E **79**, 011107 (2009).

[35] M. E. J. Newman and R. M. Ziff, Phys. Rev. Lett. **85**, 4104 (2000).

[36] M. J. Lee, Phys. Rev. E **76**, 027702 (2007).

[37] X. M. Feng, Y. Deng, and H. W. J. Blöte, Phys. Rev. E **78**, 031136 (2008).

[38] B. Nienhuis, in *Phase Transitions and Critical Phenomena*, edited by C. Domb and J. L. Lebowitz (Academic, London, 1987), Vol. 11; J. L. Cardy, in *Phase Transitions and Critical Phenomena*, edited by C. Domb and J. L. Lebowitz (Academic, London, 1987), Vol. 11.

[39] M. F. Sykes and J. W. Essam, J. Math. Phys. **5**, 1117 (1964).

[40] J. W. Essam, in *Phase Transitions and Critical Phenomena*, edited by C. Domb and M. S. Green (Academic, London, 1987), Vol. 2, p. 197.

[41] W. Zhang and Y. Deng (unpublished).

[42] H. Hu and Y. Deng (unpublished).